Optimal operation of combined wind power and energy storage in multi-stage electricity markets ☆

Guzmán Díaz[a,*], José Coto[a], Javier Gómez-Aleixandre[a]

[a] *Dep. of Electrical Engineering, University of Oviedo, Campus de Viesques, s/n, 33204 Spain*

Abstract

This paper provides a methodology to compute the optimal bidding by a wind power producer in a multi-stage market. The methodology is not restricted to the two-stage markets often reported in the literature—a day-ahead bid submission followed by an adjustment in the imbalance market. Instead, it allows studying any number of markets operating on the same dispatch hour. Particularly, this paper analyzes part of the Spanish market, covering the day-ahead, the six intraday, and the imbalance market. They are markets with different schedules, but this paper shows that by simply rearranging the market prices into a single equivalent market and employing the increments of power as bids, the calculations are visibly simplified; despite the different scope and gate closures. The methodology also includes a dynamic programming approach that relies on the equivalent market data to provide an optimal bidding sequence and its economic value when (i) uncertain prices and wind power production are considered, and (ii) energy storage is employed. As an application, the proposed methodology is employed to analyze the revenues derived by a wind power producer using ESS in the Spanish market.

Keywords: Wind power, energy storage, intraday markets, imbalance, optimality, uncertainty

1. Introduction

1.1. Motivation

Day-ahead market is undoubtedly the most known of all electricity markets. Through competitive biddings, this market produces the starting price and unit commitments for every hour of the next day. It is clearly the blueprint for the next day hour-by-hour energy dispatch. Yet, it is be followed by possibly a less-known set of cascading actions developed in specific markets and aimed at modifying the equilibrium found in that first, fundamental market. Some of these actions will be mostly economical, reflected in the participation of some of the parties in successive markets that provide the opportunity of adjusting the initial bid for either technical or speculative purposes. For instance, in Spain there are six consecutive markets of this type, named intraday markets. Other actions will have more technical content, however, intended to guaranty the feasibility and security of the power supply. For instance, after the intra-day a restrictions

☆This work was supported in part by the Spanish Ministry of Economics, Industry, and Competitivity under Grant ENE2016-80053-R.

*Corresponding author

Email addresses: guzman@uniovi.es (Guzmán Díaz), jcoto@uniovi.es (José Coto), jgomez@uniovi.es (Javier Gómez-Aleixandre)

market is launched to resolve conflicts or constraints in the day-ahead equilibrium. Similarly, the imbalance market is a final, real-time adjustment that seeks to match supply and demand. (In Spain there are indeed three related markets that fit this model, namely secondary, tertiary, and deviation management, this latter with peculiar activation. Additionally, see [1] for an excellent review on ahead and real-time market structures.)

A wind power producer may want to participate in some of these markets for technical or economical reasons. The producer may want to modify the day-ahead bid because of updates in the output power forecast or simply to take advantage of price differences through arbitrage. However, the economic value of this participation is difficult to calculate by the wind power producer. In the case of Spain, day-ahead, intraday, and imbalance markets have different durations, periods, gate closures, and rules. Also, they are managed by different operators. OMIE (Iberian Electricity Market Operator) handles the day-ahead and intraday markets, whereas the TSO, REE (*Red Eléctrica de España*, Spanish Electric Network), is in charge of the restrictions, ancillary services, and real-time imbalance markets. In addition, the behavior of the prices in these markets—and the power production in the case of the wind power producer—is subject to uncertainty.

The above situation is complicated if energy storage systems (ESS) are considered. Classically pumped hydroelectric storage and more recently CAES have been proposed in the literature as a supporting mechanism to smooth wind power fluctuations. It is a matter of deferring production to adapt the bids to the evolution of the day-ahead price or to compensate for forecasting errors.

In view of the above arguments, the practical problem that first motivates this paper is: How can a wind power producer work out the value of participating in a number of concurrent but different markets, mindful that the evolution of prices and power is uncertain? In addition, a second motivation comes from the introduction of ESS into the problem. The question in this case is: Under the same uncertain conditions, would ESS provide added advantages when operating in that sequence of markets?

1.2. Literature review

Much of the recent research in the field of wind power trading has revolved around the idea of controlling forecast error losses in the day-ahead market by modifying bid submissions in the imbalance market. A seminal work in this field was that by Conejo *et al.* in [2, Sec. 6]. Their approach built on two models and one two-stage optimization program. First, they modeled the market rules, mainly considering the existence of a balance market in which the wind power producers could adjust the day-ahead offers. Secondly, they derived ARMA models of wind speed. Those models served to generate wind power paths that in this particular case were weighted by a pair probability-price to obtain a set of scenarios. Thereafter, they proposed a stochastic two-stage stochastic program, an optimization program with recourse, in which the optimal bids and their value were obtained.

Central to this approach is the existence of a two-market settlement, which allows for the application of a two-stage stochastic program. Following this approach, different applications or studies broadened its scope. Guerrero-Mestre *et al.* concentrated on calculating the value of coordinating the offers of different farms, with recourse to the possible imbalance market [3]. Pinson *et al.* integrated forecast uncertainty

in the form of predictive distributions [4]. Their work was focused on the day-ahead market, proposing further future research on other markets with a variety of gate closures. Similarly, Shin *et al.* refined the bid behavior by introducing information related to the correlation between wind speed and electricity prices rather than using only marginal distributions [5] . In [6], the focus was on the difference between day-ahead and real-time locational marginal prices. Again they investigated how to benefit from deviations in two different markets. In [7] the aim was to detect whether directly bidding to the balance market was interesting in the Nordic market. The answer was positive, but only in the case of a two-price balancing mechanism (which we have used in our research and explain later). In [8] the authors refined their previous research to introduce risk as decision factor, resulting in different degrees of market power.

On the whole, these are instances of a common approach in which a two-stage market permits contract recourse [9]. But an inherent limitation to this approach is that its expansion to three or more markets becomes complicated. This is a drawback, since in practical terms the adjustment in intraday markets may be more profitable than updating the production in the imbalance market [10].

The problem becomes more complicated when the producer employs ESS to mitigate wind power uncertainty. This has been addressed in proposals based on classic pumped hydro [11, 12], more recently compressed air energy storage (CAES) [13], or some innovative approaches such as underwater CAES [14] to cite some. In the case of [11], the authors followed the method in [2] and analyzed the coordinated and uncoordinated operation of wind power and ESS. De la Nieta *et al.* also analyzed the profitability of joint versus uncoordinated operation of pumped hydro and wind (concluding that coordinated operation is preferable) in day-ahead and imbalance markets [12] . In [15], the authors employed a two-stage stochastic program to analyze the case of a wind and solar power producer, whose production was supported by ESS. In [16], thermal storage and pumped hydro were included as a support to wind power, again in a two-market analysis and using a two-stage stochastic program. In this case, the ESS was formulated as a sequence of constraint equations that reflected the consecutive states of charge of the storage.

The possibility of a wind power producer bidding in more than two electricity markets using ESS has been addressed to some extent in the literature. Berrada *et al.* [17] studied several sources of revenue in a wind-ESS system: day-ahead and regulation markets. However, their approach was deterministic, of application to historical data. In [18], the authors also included the intraday markets, but in a different scope. They wanted to know how ARMA-based forecast accuracy of wind power affected the profitability.

1.3. Aim and contributions

This paper describes the methodology and application of a group of techniques for computing the economic value of bidding in a number of sequential electricity markets, under uncertain power production and prices, with the added support of energy storage. The argument in this paper is that different markets targeting the power dispatch of each hour of the next day can be treated as one single market and the bid be optimized by means of a dynamic program that allows for the incorporation of complex decisions at the bidding stage.

This paper covers three topics related to the calculation of that economic value. First, it reports on the application of dynamic linear models (DLM) to characterize uncertain prices and wind speed. These are

structural models that can be tailored to different time series characteristics. This paper provides evidence that the use of DLM in this specific area is advantageous, since the different electricity market prices can be treated similarly, at the stage of model calibration, if the DLM structure is chosen as a function of each market rules (mainly duration and periodicity). In other words, one basic model can be applied to substantially different markets, thus simplifying the model specification.

Secondly, this paper describes the procedure we followed to handle the different market prices. Disparate market schedules and activities over different periods difficult the calibration of price models and the specification of optimization programs. To confront these problems, we completely altered the processing of the different market data by first treating them as continuous time series of different lengths, which proved to facilitate the DLM calibration.

Finally, we developed an algorithm that enables the determination of the optimal bidding and its value for a wind power producer employing ESS. The algorithm relies on dynamic programming (DP) and on the particular redefinition of the prices and power referred to in the previous paragraph. Khalid *et al.* recently employed a DP approach to solve the problem of finding the optimal dispatch of a battery-based wind power system [19]. They concentrated on the use of a receding horizon policy, which is different to the optimal switching policy that we have followed in our work. But the advantages of the DP approach that they summarized and demonstrated in their paper—it is efficient, allows for non-linear problems, and guarantees a global optimum—are of application to our work as well. An advantage, also, is that this approach offers the flexibility of evaluating complex decisions at each individual step. The cost of a decision is encapsulated into one payoff function, which receives the information about the price, the available power, the stored energy, a prospective decision for a given hour, and produces a scalar value of the cost. This is compared with other options at the same hour to produce the optimal solution, which will be memorized, all in a simple and direct way.

To our best knowledge no study has investigated the application of stochastic dynamic programming to the valuation of wind-ESS participation in multi-stage markets. Our work is focused on the activity of a single wind generator, as an instance of a party subject to uncertainty in power production. Generalization to other types of generation and/or number of generators is straightforward. As an application example, this paper shows how the proposed approach is appropriate to solve the problem of optimal bidding in the Spanish multi-stage market.

1.4. Document structure

This paper is divided into four more sections. Next section explains the problem, and describes the methodology and the data employed. It also depicts the conducted case analysis. Then, the third section is devoted to show the results obtained from the different steps of the presented approach. The interpretation of those results is conducted in the fourth section. Finally, the last section presents the conclusions

2. Methodology

2.1. Problem characterization

An agent participating in the Spanish electricity market can intervene in several different submarkets, with distinct spans and gate closures. This is summarized in Table 1. The day-ahead market held on the

Table 1: OMIE's market structure.

	bidding		delivering	
	opening	closure	starts	duration
day ahead	10:00 $(D-1)$	12:00 $(D-1)$	00:00 (D)	0
intra-1	16:00 $(D-1)$	18:00 $(D-1)$	20:00 $(D-1)$	28
intra-2	21:00 $(D-1)$	22:00 $(D-1)$	00:00 (D)	24
intra-3	01:00 (D)	02:00 (D)	04:00 (D)	20
intra-4	04:00 (D)	05:00 (D)	07:00 (D)	17
intra-5	08:00 (D)	09:00 (D)	11:00 (D)	13
intra-6	12:00 (D)	13:00 (D)	15:00 (D)	9

previous day $(D-1)$, accounting for the operation of the power system the next day (D), is followed by several adjustment or intraday markets. In Spain, there are six intraday markets. They serve to reposition the bids of those agents who cannot fulfill their commitments in the day-ahead market because of unexpected events or bad forecast. But the adjustment also serves as a way of adopting short positions, selling and buying energy in a speculative way when volatility is high. These seven markets are managed by the market operator, OMIE (Electricity Iberian Market Operator), in charge of managing the Iberian Peninsula transactions (Portuguese and Spanish).

Following these seven markets, the system operator REE is in charge of the real-time balancing, which amounts to at least the launching of an additional imbalance market. The prices in this market are asymmetric, depending on the position of the participant at the time of delivery and the system balance. If there is an excess of generation in the system, then the price paid is

$$\begin{aligned}\lambda_t^+ &= \min(\lambda_t^{\mathrm{DA}}, \lambda_t^{\mathrm{DN}})\\ \lambda_t^- &= \lambda_t^{\mathrm{DA}},\end{aligned}$$

where λ_t^+ is the price received for higher production than scheduled, λ_t^- for lower production, λ_t^{DN} the downward regulation price and λ_t^{DA} the day-ahead price, with $\lambda_t^{\mathrm{DN}} \leq \lambda_t^{\mathrm{DA}}$. This means that the excess generation is remunerated at a price lower than the day-ahead clearing-market price (see Fig. 1). If by contrary there is a deficit of generation, then the prices involved are:

$$\begin{aligned}\lambda_t^+ &= \lambda_t^{\mathrm{DA}}\\ \lambda_t^- &= \max(\lambda_t^{\mathrm{DA}}, \lambda_t^{\mathrm{UP}})\end{aligned}$$

If E_t^{DA} is the energy offered by the agent or balance responsible party (BRP) for hour t of day D in the day-ahead market—which may or not be later adjusted in the intraday markets—and the energy delivered at that same hour is E_t, then the payment is summarized in Fig. 1. Particularly, when imbalances are accounted for, the line is broken at $(E_t^{\mathrm{D}}, \lambda_t^{\mathrm{DA}} E_t^{\mathrm{D}})$, ensuing in a piecewise line that may vary its slope *in one* of the two sides defined by that point:

- $R_t = \lambda_t^-(E_t - E_t^{\mathrm{DA}}) + \lambda_t^{\mathrm{DA}} E_t^{\mathrm{DA}}$, to the left of the point (i.e., $E_t > E_t^{\mathrm{DA}}$); and
- $R_t = \lambda_t^+(E_t - E_t^{\mathrm{DA}}) + \lambda_t^{\mathrm{DA}} E_t^{\mathrm{DA}}$, to the right of the point (i.e., $E_t < E_t^{\mathrm{DA}}$).

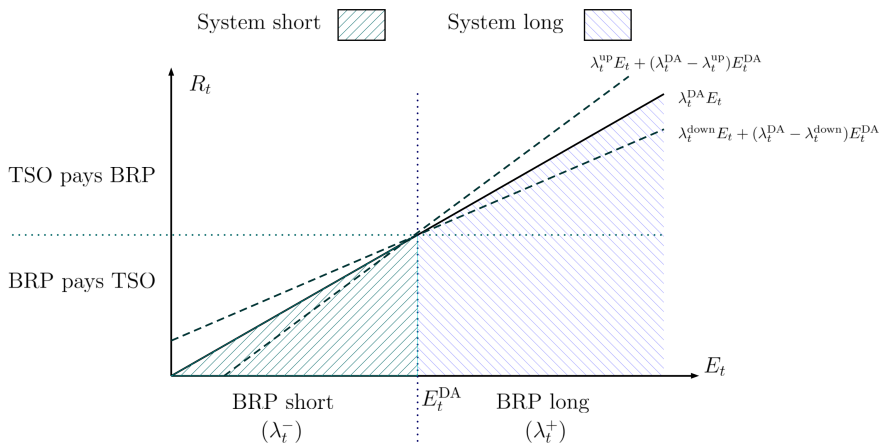

Figure 1: Imbalance pricing.

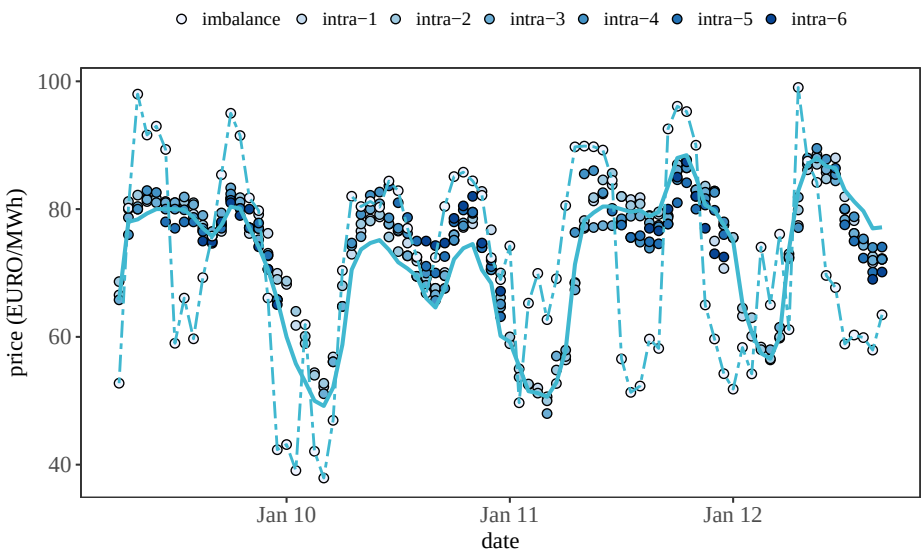

Figure 2: Three-day sample of prices in January 2017. The day-ahead and the final imbalance markets are highlighted in thick continuous and thin dashed lines, respectively

As a result of this market structure, an agent intervening in the Iberian power markets observes at least the prices shown in Fig. 2.[1] Each hour, a generator has the opportunity to participate in a varying number of markets, ranging from four during the early hours of the day (0:00 to 5:00) to eight markets, starting at 16:00 hours. During the period from 5:00 and 16:00, the number of active markets is progressively increased. The activity is readily observed in Fig. 2 as a function of the number of points for each hour. Particularly, this representation is useful for understanding the reason for this complex structure. It is at the time at which the system is more stressed, the peak hours, when the the number of active markets is larger.

It is necessarily to be noted that an agent participating in the energy trade for a given hour does so

[1]We do not consider additional pricing mechanisms that include for instance technical restrictions, ancillary services, etc.

at different times in the $D-1$ and the D days (see Table 1). This means that an agent can participate in eight markets concerning the dispatch at for instance 8:00 p.m. But the bids to these eight markets must be presented sequentially through eight consecutive steps, starting at 11:00 a.m. of day $D-1$ and ending at practically the delivery hour of day D. When the participation is scheduled for 2:00 a.m., however, only four markets are available. Unfortunately, this complicates the economic valuation of the participation under optimal decisions and uncertainty.

2.2. Methodology

In what follows we detail the methodology we used to analyze the characteristics of an optimally switched ESS supporting a wind power producer in the multi-stage Spanish electricity market. The key aspects of this methodology can be listed as follows:

1. We downloaded the price data from OMIE's repository. It can be accessed on [20]. These data come in a proprietary format and are stored in files corresponding to separate days. As a consequence, intensive preprocessing is needed to adapt the data to common time series spanning several days. We also employed data from NREL's repository on [21] as a source of wind speed time series.
2. We subsequently specified and calibrated different models for each market. Though structurally different, all the models were developed using the same dynamic linear formulation, as explained in [22]. We proceeded in the same way with wind speed data.
3. We simulated the models to obtain K samples representing possible evolutions of the eight market prices. These simulations implied reconstructing the inactive periods of the markets following the second intraday in the hourly sequence, since market inactivity was removed in the previous phase to facilitate calibration. The simulations were followed by a specific rearrangement of the data to summarize the $8 \times K$ samples into only K samples.
4. We developed an optimization algorithm based on stochastic DP to compute the optimal switching sequence of the ESS along all the markets.
5. Finally, we conducted a multiple regression analysis to obtain conclusions about how the incorporation of ESS to support a wind power production affects the producer income and participation in the different markets.

2.2.1. DLM specification and calibration

Dynamic linear models (DLM) expand the scope of linear regression models. In a linear regression model the relationship between a scalar response variable and one or more predictor variables is modeled as $y_t = \boldsymbol{\beta}^t \mathbf{x}_t + \varepsilon_t$, with ε_t a residual error, and where the parameter vector $\boldsymbol{\beta}$ remains constant over the considered sampling period. Differently, a DLM is a linear state-space model of the form

$$y_t = \mathbf{F}_t \mathbf{x}_t + \mathbf{v}_t, \quad \mathbf{v}_t \sim \mathcal{N}(0, \mathbf{V}_t), \tag{1}$$

$$\mathbf{x}_t = \mathbf{G}_t \mathbf{x}_{t-1} + \mathbf{w}_t, \quad \mathbf{w}_t \sim \mathcal{N}(0, \mathbf{W}_t), \tag{2}$$

in which the regression parameters are not necessarily constant but time-varying, and indeed they are treated as the system states. $\mathbf{x}_t$ is the state vector or unobserved states that are related to previous realizations by means of the transition matrix $\mathbf{G}_t$; and the operator $\mathbf{F}_t$ translates the combination of hidden states

into the observation y_t at time t; either price or wind speed in our work. Both observation and transition evolutions are driven by stochastic inputs captured by the vectors $\mathbf{v}_t$ and $\mathbf{w}_t$, with Gaussian distributions having covariance matrices $\mathbf{V}_t$ and $\mathbf{W}_t$.

The structure of the model—which includes the underlaying characteristics of trend, seasonality, ARMA processes, and others—can be conveniently defined as a sum of terms that in (1) and (2) result in matrices formed by stacking components (see for instance [22, Sec. 3.2]). Additionally, when the system structure is time-invariant, as we assumed in this work, the matrices in (1) and (2) are constant and depend on parameters that can be encapsulated into a vector $\boldsymbol{\theta}$. Kalman filter can then be employed to estimate $\boldsymbol{\theta}$ from the process observations by maximizing the log-likelihood as explained in [22, Sec. 7.2].

The final model is obtained as a result of a trial and error process, in which a prospective underlying structure is proposed a priori through $\mathbf{G}$ in (2), with unknown parameters. These parameters are determined by calibrating the model using the Kalman filter. And finally, the validity of the calibrated model is assessed by analyzing the normality of the residuals and their lack of autocorrelation. If this assessment is not positive, another model is proposed and the procedure repeated.

Prior to calibrating the series, we always proceeded with a normalization of the data. Other authors have also employed this kind of data pre-conditioning, alluding to its benefits at the time of calibrating. The techniques reported in the literature are various. For instance, an early favored one was the Box-Cox transformation, which was employed to normalize wind speed data in [23, 24]. It is a well-known logarithmic-power transformation that provides the normalization as a by-product of the stabilization of the variance. But recently, Nataf's transformation has been more popular [25, 26, 27, 28, 29, 30]. This transformation is obtained in a two-step procedure that first tranforms the original time series into an uniformly distributed stochastic process, which then is converted into a normally distributed variable. The first transformation is obtained by means of the inverse cumulative distribution function, $F_X^{-1}(x_t)$. The second transformation employs the standard Normal cumulative distribution function, $\Phi(\cdot)$. To transform the stochastic variable observations, x_t, we applied

$$x'_t = \Phi(F_X^{-1}(x_t)). \tag{3}$$

There are not restrictions on the specification of $F_X(x_t)$. It can be parametric or not. Accordingly, because of its speed and good results, we employed the kernel estimation function proposed by Botev *et al.* in [31].

After the model is validated, the model can be simulated and, thereafter, reverted to the original space simply by passing the simulated series through the expression

$$x''_t = F_X(\Phi^{-1}(x'_t)). \tag{4}$$

2.3. Optimization program

To obtain the optimal charge/discharge sequence of an ESS supporting the wind power production, and subsequently value the income obtained following that optimal sequence, we developed an optimization algorithm based on the optimal multiple stopping theory for valuation of swing options [32, Sec. 4].

Swing options can be viewed as an extension of American options. These latter are contracts that allow the holder to buy or sell a specified underlying asset, on or before a predetermined expiration date.

The optimization programs related to this type of problems analyze and find the optimal stopping times that ensure a maximum profit from exercising the option. Swing options are an extension, in which the option exercise is not limited to occur once, but it can be exercise several times over the life of the contract. Our approach relies on adapting the swing options theory to the ESS problem, in which the option of exercising (buy or sell) is translated into the option of charge/discharge, with an added characteristic of memorization.

The state of the ESS can be defined by its state of charge (SoC) at each time t in the time interval $[0, T]$, where T is the programming horizon. We discretized the SoC into L levels, and hereafter ℓ_t denotes the SoC in that discretized space at time t. At a given instant, the SoC depends on the past history of the ESS operation. Over the operation period the SoC would have followed a path that can be summarized as $\boldsymbol{\ell} = (\ell_t)_{t\in[0,T]}$, driven by a set of decisions (to charge/discharge) that can be summarized in $\mathbf{u} = (u_t)_{t\in[0,T]}$. The aim of the optimization program is to find the optimal path, $\boldsymbol{\ell}^*$, that would provide maximum profit from operation in all the considered markets.

The value of the profit obtained from operating in the markets can be written as

$$J(\mathbf{X}_0, \mathbf{u}) = \mathbb{E}\left[\int_0^T \Pi(\mathbf{X}_t, u_t)\,\mathrm{d}t + \zeta(\mathbf{X}_T, \ell_T)|\mathcal{F}_t\right] \tag{5}$$

That is, the value of exerting the control actions $\mathbf{u}$ over the period $[0, T]$ is made up of two terms. The first term, $\Pi(\cdot)$, is the payoff at time t obtained from exerting the control action u_t subject to the price and power information encapsulated in the vector $\mathbf{X}_t$. The second term, $\zeta(\cdot)$, assess the residual SoC at the end of the period. Additionally, because both terms must be evaluated within a framework defined by the uncertainty of prices and wind power, the result is the expected profit, which is conditional on the flirtation $\mathcal{F}_t$ that affect the decision process. The filtration $\mathcal{F}_t$ summarizes the information available at the time of decision [33, §5.1].

To solve this problem, the considered period can be discretized into N intervals, which allows to apply (5) sequentially or recursively. Particularly, the profit in a generic interval $[k, k+1]$ becomes simply

$$J(\mathbf{X}_k, u_k) = \mathbb{E}\left[\Pi(\mathbf{X}_k, u_k) + \zeta(\mathbf{X}_{k+1}, \ell_{k+1})|\mathcal{F}_k\right]. \tag{6}$$

In this interval, we have to compute the payoff ensuing from exerting a control action u_k, which is simply a matter of appropriately define a payoff function that reflects the cost and benefits of the decision to operate (or not) the ESS. Secondly, we have to compute the residual value $\zeta(\cdot)$. But importantly, if we proceed backwards—starting at the last interval in the considered period—we can easily compute that residual value as

$$\zeta(\mathbf{X}_{k+1}, \ell_{k+1}) = J(\mathbf{X}_{k+1}, u_{k+1}) \tag{7}$$

In this way, the optimization is conducted through simple subproblems—one at each ingterval—and the results are stored (memoization) to be passed to the previous interval in the time sequence. At each step, the optimization comes down to calculating the optimal trade-off between the payoff, $\Pi(\mathbf{X}_k, u_k)$, obtained from operating the ESS and the residual value, $\zeta(\mathbf{X}_{k+1}, \ell_{k+1})$, that occurs when that action u_t will leave the ESS with a charge ℓ_{k+1}. At each step, the residual value is a representation of what lies ahead.

The payoff function maps to a scalar value of income the participation in different markets. To define it without complicating the problem, we decided that this payoff function would be calculated from power increments. The power dispatch only occurs once every hour, despite the existence of several trading markets for that same hour. The number of markets is variable, depending on the hour of the day. Besides, the actual bid is only done in the day-ahead, with the rest of the markets employed to make corrections. So if the payoff were to be calculated using the power bid in each market, the payoff function should have to have access to a market code for each bid to correctly compute the profit. This would complicate passing arguments to the function, because the price series is a single aperiodic series, made up of prices of ordered markets. Therefore, to avoid passing that information to the payoff function and thus keep it simple, we modified each sample of power at the time of forming the single-market price series. The series would be differentiated in the adjustment markets to account for corrections. This showed to be much simpler and effective, because the payoff function in such a case is the product of the price (regardless of the market type) times the increment (in case of non-day-ahead markets) of the difference between the wind power and the stored energy. That is, it is simply the product of price times the dispatched (i.e. non-stored) power.

By proceeding with this sequence of optimization of subproblems, eventually the optimal switching sequence $\mathbf{u}^*$ is obtained, with the value of operation equal to

$$V(\mathbf{X}) = \arg\min_{\mathbf{u}} \sum_k J(\mathbf{X}_k, u_k). \tag{8}$$

The obtained sequence $\mathbf{u}^*$ is optimal because an optimal policy has the property that whatever the initial state and initial decision are, the remaining decisions must constitute an optimal policy with regard to the state resulting from the first decision [34, Ch. 3].

Regarding the uncertainty on $\mathbf{X}_k$, we introduced it in two ways. First, we conducted the optimization in a Monte Carlo framework. As explained in a previous subsection, we simulated the calibrated structural models to obtain K samples (time series) of wind speed and prices. These samples were encapsulated in $\mathbf{X}$. Second, we avoided the perfect foresight error—that is, a perfect knowledge of what is going to come at each time step—by estimating $\zeta(\mathbf{X}_{k+1}, \ell_{k+1})$ at each step as a stochastic residual value with a expectation conditional on the observation of $\mathbf{X}_k$. This method was first introduced by Longstaff and Schwartz in [35] in the field of optimal stopping calculation. Their paper throughly explains the basis of this procedure.

All this procedure can be efficiently computed by means of matrix operations. At each step, we defined a payoff matrix of size $K \times L$ that included the payoff from changing the SoC to all allowed levels in all possible realizations of $\mathbf{X}_k$ obeying a prospective decision. This matrix was summed to a second matrix, which stored the conditional expectation of the accumulated residual values, producing a matrix of the cost of exerting that decision, which we have called $J(\mathbf{X}_t, \mathbf{u})$ above. Constraints in the ESS capacity are readily defined by assigning a very large cost (infinite) to levels outside limits; and the maximum charge/discharge power can also be easily defined by bounding the values of $\mathbf{u}$. At each step we followed this procedure with all possible values of $\mathbf{u}$. Eventually, it is a matter of comparing all the cost matrices to obtain the optimal decisions for each realization of $\mathbf{X}_k$. We implemented the routine in R, requiring no external optimization libraries.

As a result of the algorithm, the optimal bidding and charging/discharging sequence can be obtained

and the payoff calculated. To investigate the correct calculation of the operational sequence (charging/ discharging sequence of the ESS), we compared our results to a simple problem solved by means of an interior-point optimization algorithm. The problem was defined as

$$\min_{\mathbf{u}=(u_1,\ldots,u_T)} \mathbf{p}^t\mathbf{u} \tag{9}$$

$$\text{s.t.} \quad \sum_{k=1}^{T} u_k = 0, \tag{10}$$

$$\sum_{i=1}^{k} u_k = \ell_k, \tag{11}$$

$$0 \leq \ell_k \leq 1, \quad \forall k \in [1, T]. \tag{12}$$

This is a problem of reduced complexity in which a price time series, the vector $\mathbf{p}$ is employed as an input to find the optimal energy arbitrage by means of an ESS. It computes the optimal switching sequence employing as many decision variables as investigated intervals; in this case T. This number of decision variables is multiplied by the number of paths or samples of $\mathbf{p}$. This means that if K simulations of $\mathbf{p}$ are employed, the problem will have $K \times T$ decision variables. Our validation of the ESS operation only employed $K = 1$ and $T = 100$. Both approaches, our dynamic programing and the interior-point, produced the same operation sequence.

In a 64-bit Intel(R) Core(TM) i7-4712HQ CPU 2.3GHz, with double core and 6 GB of installed RAM, optimizing the ESS switching sequence of $K = 100$ samples of a one-month period (744 hours), employing a discretization of the SoC into 100 levels, and accounting for the operation in the eight electricity markets, the calculation took around 4 seconds.

2.4. Case analysis

In order to assess the value of bidding in successive adjustment markets using (or not) energy storage, we defined a series of scenarios. They were:

(1) Base case. All the other cases were some variations with respect to what is described next for this scenario:
   - Wind turbine Vestas V47-660 (660 kW); see for instance [36].
   - Wind profile corresponding to NREL site no. 1775.
   - No support by energy storage provided.
   - Price data set corresponding to January 2017.
   - The wind power forecast did not improve as the delivery time approached.

(2) The wind turbine considered was the Vestas V44-600 (600 kW). Compared to the V47-660, the V44-600 has a narrower production range. The cut-in speed is 5 m/s and the cut-off 20 m/s (compared to 4 m/s and 25 m/s of the V47-600).

(3) Wind speed distribution corresponding to NREL site 25212. It features lower mean wind speed, as well as higher skewness.

(4) Wind speed forecast uncertainty was progressively revealed as the delivery time approached.

(5) Price distribution obtained from April 2017 dataset.

(6) A 1200-MWh, 100-kW ESS was included.

(7) A 1200-MWh, 100-kW ESS was included, to analyze data from April 2017.

(8) A 1200-MWh, 100-kW ESS was included, to analyze uncertainty.

All in all, we tried to summarize the exposure of a wind power producer to a sequential market under conditions that depended on the wind regime, month, wind turbine, and, above all, the use of ESS. We tested all scenarios by simulations comprising 100 samples of simulated wind speed and prices (of the seven markets) that spanned a one-month period. To classify, assess, and analyze the consequences of participating in these sequential markets, we eventually conducted a multiple linear regression of the income received from optimal operation on the prices of the different markets. We acknowledge the limitations of this approach because the fit of the regression model is far from satisfactory (see below). But the aim of the regression analysis was not to model such complex interactions—for which far more complex machine learning procedures should have to be applied—but to infer conclusions about the gains obtained by introducing ESS.

3. Results

A sample of the results obtained by splitting the original series into structural components using the DLM approach is shown in Fig. 3, representing the prices of the *incomplete* fifth intra-day market in October 2017. Particularly, this market covers the period 11 a.m. to 23.00 p.m. We removed the inactive hours (from 0 though 10 a.m.), thus producing the continuous representation shown in Fig. 3, which served to facilitate the calibration procedure. This is the reason why the number of samples shown in Fig. 3 are $13 \times 31 = 403$ samples rather than the full coverage of the day-ahead, the imbalance, or the first two intra-day markets, which would show $24 = 744$ samples.

A sample of the results obtained after analyzing the standardized residuals is shown in Fig. 4. It corresponds to the residual content after calibrating the series depicted in Fig. 4. These results were consistent across all the series analyzed, regarding the autocorrelation of residuals. In all the series the residual autocorrelation was within the confidence band of 95%, with negligible exceptions. As for the normality assumption assessed by the quantile-quantile plot, on the right panel of Fig. 4, the normality of the residuals is corroborated. In other cases, however, the plot would show more heavy tailed distribution.

Fig. 5 presents the evolution of prices obtained after simulating the structural DLM for a three-day period. The day-ahead (top) and imbalance (bottom) markets are complete, meaning that they span the 24-hour period each day; with the difference that they take place in the $D - 1$ and D day, respectively. The simulation of the imbalance market combines the positive and negative positions into a unique series, which particularly oscillates around the day-ahead market price. Differently, the 4th intra-day market (middle plot) is incomplete. The simulation was continuous (without the gaps) because we employed a continuous price series without the inactive-market gaps to calibrate the model. So later we had to reverse

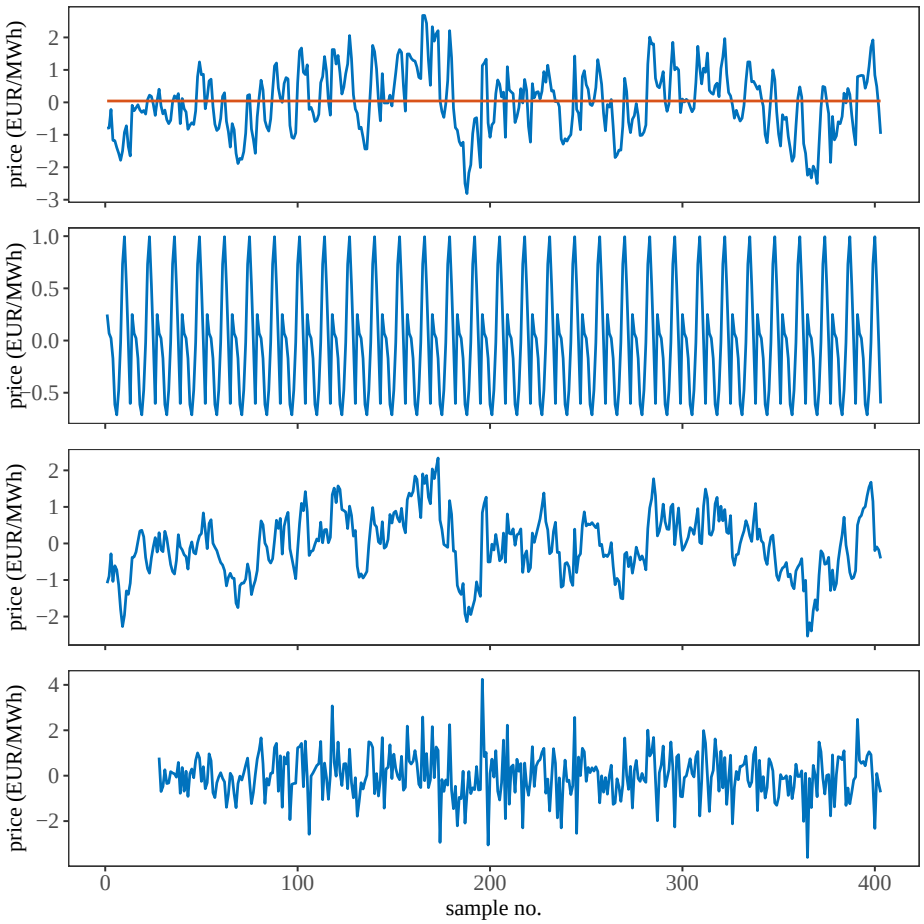

Figure 3: Decomposition of the 5th intra-day market price, October 2017. From top to bottom: Original time series and trend component, seasonal component, ARMA component, and residuals. All values are presented after normalization by means of the inverse normal transformation.

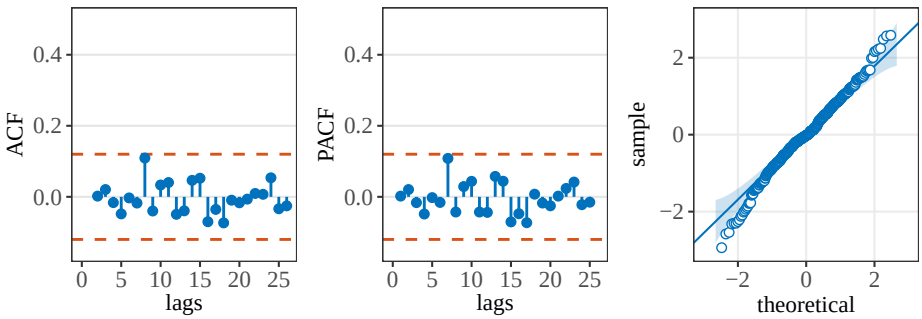

Figure 4: Residual analysis after the calibration of the series in Fig. 3. Left: autocorrelation function. Center: partial autocorrelation function. Right: quantile-quantile plot. The confidence band of 95% is shown in the three cases.

the procedure and introduce the gaps before combining the eight markets into one single market with correct sequence of prices. These gaps, of increasing length, occur in intra-day markets fourth, fifth, and sixth. Note also that vertical axes have different bounds in the three panels, because the volatility of the markets

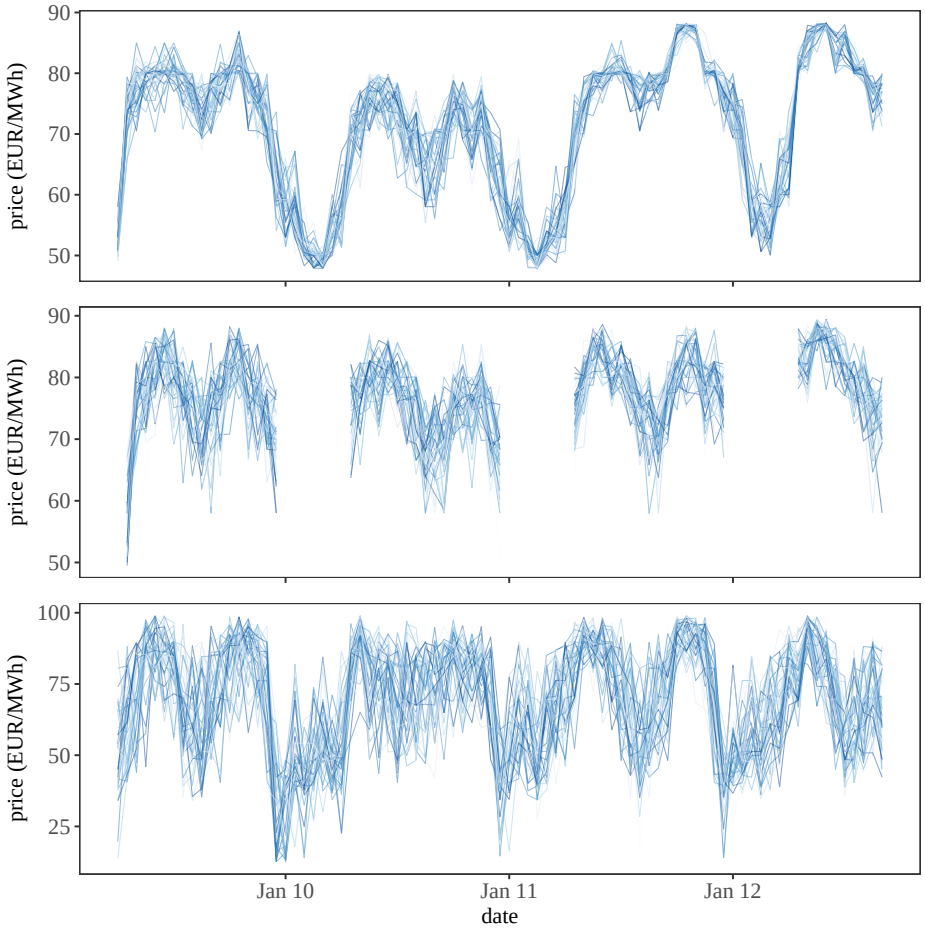

Figure 5: Simulation of 50 samples of prices: day-ahead (top), fourth intraday (middle), and combined positive and negative imbalance (bottom) markets.

are visibly different. Finally, each sample of these simulated market prices is sequentially combined, along with the non-represented five intra-day markets, to produce the representation of a unique market price as shown in Fig. 8.

By using the same structural DLM approach, we calibrated and simulated wind speeda from NREL Western Wind Data Set [21]. We selected several wind profiles from this data set, with different probability distributions. In this paper, we present only the results from sites with codes 1775 and 25212, which differ markedly in their probabilistic features. Site 1755 showed higher scale and shape parameters when fitted to a Weibull distribution. This means that the average wind speed was higher than that of site 25212, since the scale of Weibull distribution can be considered an approximation to the mean wind speed $\bar{w}_i$ as $c \approx \frac{\bar{w}_i}{\Gamma(1+1/k)}$; see for instance [37, 38]. Additionally, for shape values $k > 1.7$, the result $\Gamma(1 + 1/k) \approx 0.89$ is almost constant. For shapes around 1.5 and 2, the smaller the shape, the heavier the tail. Therefore, site 25212 showed a less constant wind speed. Fig. 6 shows a ten sample draw from the model fitted by the DLM method proposed above.

Fig. 7 summarizes the mean value and volatility of the eight Spanish markets four months apart. It

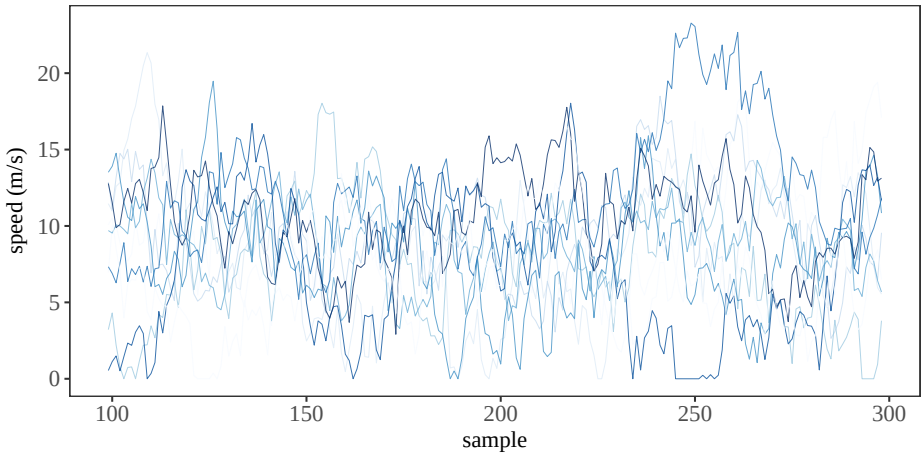

Figure 6: Simulation of 10 samples of wind speed. NREL site id. 1775.

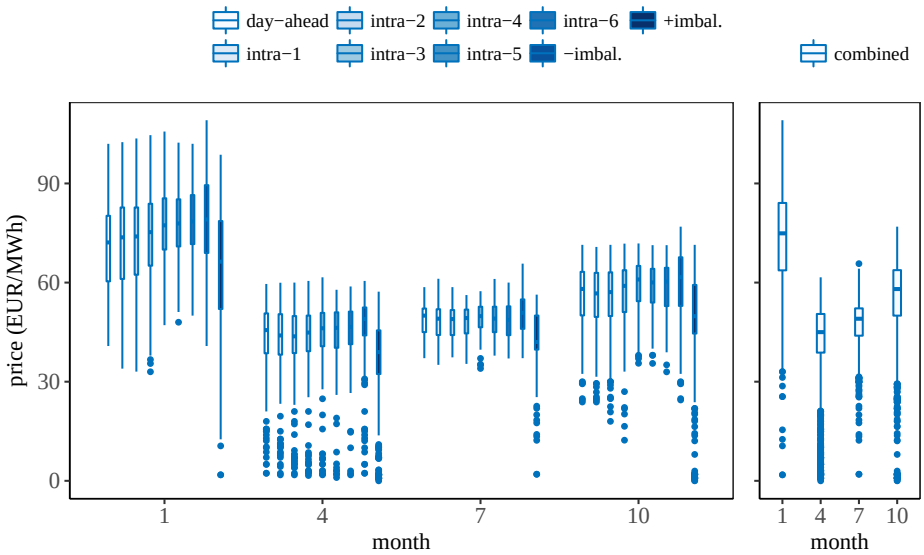

Figure 7: Distribution of prices of Spanish electricity markets (left) during four selected months of 2017, and proposed combination into one single market (right).

provides a classification of the different price structures faced by market party in Spain, depending on the year season, by means of Tukey's plots describing the quartiles and outliers of the distributions. There are nine boxes each month because imbalance prices appear individually split into negative and positive position prices. Not all boxes refer to the same number of samples as a consequence of the inactivity of some of the markets. Thus for instance, the distribution corresponding to day-ahead market prices is obtained from 744 realizations, whereas for the sixth intraday only 279 observations are available. This has direct implications on the combined distribution, as we explain later. The plot in the right panel summarizes the distribution of the combined time series following the procedure of sequencing the markets each hour.

Fig. 8 shows the market price sequence and the bidding policy resulting from sequencing the eight

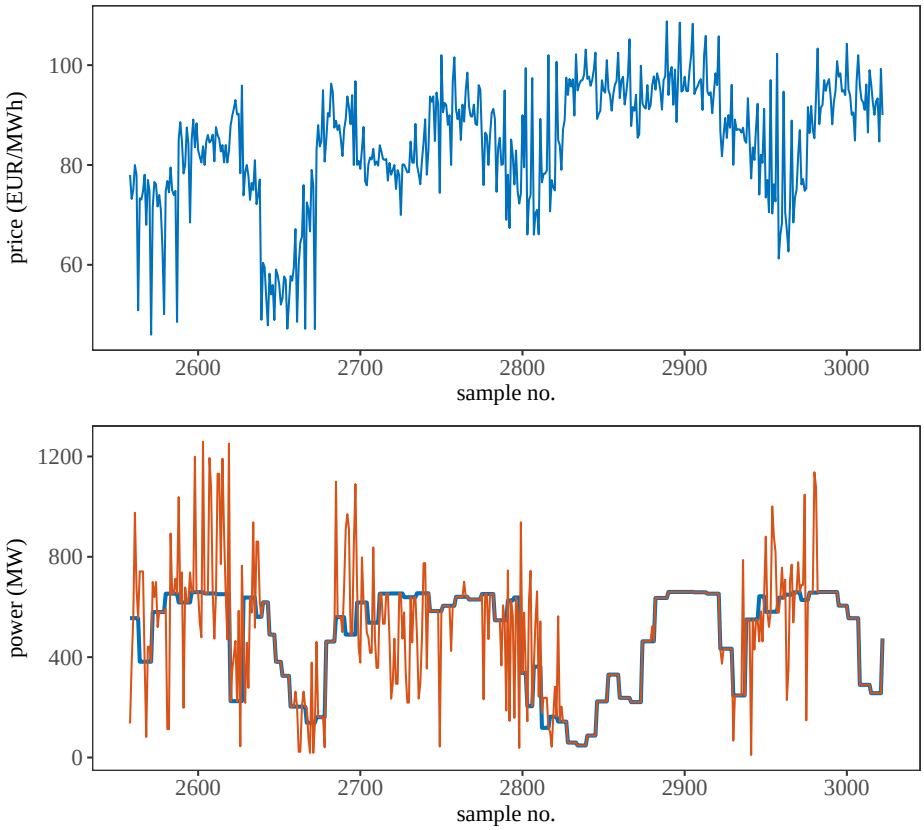

Figure 8: Top: Combined price data corresponding to Omie's seven markets and REE's imbalance market in January 2017. Bottom: Power bidded by 660-kW wind generator without (thick, blue line) and with ESS support (thin, red line). The top panel data is from a sample of a simulation of the eight markets.

markets. On top, the prices are shown, with sharp spikes corresponding to the more volatile imbalance market repeating their occurrence at variable-length intervals. The combination of complete (spanning 24 hours) and incomplete (spanning *less* than 24 hours) intra-dy markets make the plot aperiodic, with different lengths of time between the visible spikes. Below, two bidding policies are shown as a result of the application of the proposed algorithm. The thick line stands for the maximum forecast production that the generator offers in the market. The maximum value, 660 kW, was the rated power of the Vestas V47-660 generator. The thin line depicts the optimal bidding policy when a 600-kW, 1200-kWh ESS was added to support the operation of the wind generator. In this case, the maximum value reached 1200 kW, which is the added bid of the wind generator at rated power and the ESS maximum discharge. The fact that the thick line is stepwise, compared to the ESS-supported case, is because in the represented case the wind generator submitted the same power forecast across the eight markets, each hour of the delivery day. This does not happen when the uncertainty in the forecast is progressively revealed as the delivery time approaches, and it generally does not occur when the ESS is used. In any case, the income is calculated as the product of the power difference between two consecutive markets within the same hour times the price of the second of those two markets. This means that the constant power observed in the thick line of

Fig. 6 is interpreted by the algorithm as a null payoff when it occurs within the same dispatch hour.

Table 2: Descriptive statistics of the linear regression analyses.

	(1)	(2)	(3)	(4)	(5)	(6)	(7)	(8)
day-ahead	0.440***	0.317***	0.252***	0.439***	0.401***	0.382***	0.852***	0.376***
	(0.043)	(0.040)	(0.048)	(0.043)	(0.029)	(0.057)	(0.042)	(0.057)
intra-1	−0.093**	−0.082**	−0.100**	−0.101**	0.005	0.119**	−0.102***	0.118**
	(0.044)	(0.041)	(0.048)	(0.044)	(0.019)	(0.058)	(0.028)	(0.058)
intra-2	0.009	0.041	0.060	0.019	0.017	1.042***	−0.046	1.047***
	(0.056)	(0.052)	(0.062)	(0.056)	(0.025)	(0.074)	(0.036)	(0.074)
intra-3	0.036	0.071**	0.032	0.036	−0.023	−0.415***	−0.139***	−0.414***
	(0.037)	(0.034)	(0.041)	(0.037)	(0.025)	(0.049)	(0.036)	(0.049)
intra-4	−0.00002	−0.020	−0.010	0.002	−0.034*	−0.381***	−0.115***	−0.381***
	(0.035)	(0.033)	(0.039)	(0.035)	(0.019)	(0.047)	(0.027)	(0.047)
intra-5	0.015	0.009	−0.006	0.012	0.018	−0.413***	−0.174***	−0.414***
	(0.037)	(0.034)	(0.041)	(0.037)	(0.022)	(0.049)	(0.032)	(0.049)
intra-6	0.035	0.034	0.040	0.035	0.018	−0.196***	−0.112***	−0.193***
	(0.026)	(0.024)	(0.028)	(0.026)	(0.016)	(0.034)	(0.023)	(0.034)
imbalance	0.022	0.025*	0.037**	0.020	0.013	0.329***	0.260***	0.331***
	(0.015)	(0.014)	(0.016)	(0.015)	(0.009)	(0.019)	(0.013)	(0.019)
Constant	−4.781***	−5.347***	−3.891***	−4.775***	−0.640	−0.682	2.585***	−0.768
	(1.321)	(1.222)	(1.451)	(1.324)	(0.618)	(1.743)	(0.887)	(1.742)
Adjusted R^2	0.060	0.050	0.022	0.059	0.082	0.133	0.106	0.133
RSE (df = 13491)	20.380	18.853	22.377	20.425	11.754	26.878	16.889	26.876
F (df = 8; 13491)	107.906***	90.194***	38.177***	107.319***	151.669***	260.093***	200.062***	260.807***
Income (k€/year)	138.9	112.2	88.6	138.2	82.4	141.1	84.5	140.2

Note: *p<0.1; **p<0.05; ***p<0.01

Finally, Table 2 lists the descriptive statistics of the multiple regression analyses, following the eight scenarios proposed above. It also reports the mean value of income in each case. This is not a result of the regression analysis, but directly from the optimization routine by evaluating the payoffs following the optimal path of each simulated case and computing the unweighted mean. It is shown in this table for brevity and convenience.

4. Discussion

The calibration of prices and wind speed using the structural models depicted by Durbin and Koopman in [22] has shown to be satisfactory. In the case of prices the importance of seasonality and autocorrelation is emphasized through the decomposition into structural components (see the sample decomposition in Fig. 4). The decomposition show the importance (amplitude) and patterns of the underlying components. In the case of prices, it is readily observed the role of periodic positive asymmetric spikes in making up the original signal. This does not happen in the case of wind speed, where the seasonal component is almost negligible. In all cases, the autoregressive component had a fundamental role, highlighting the dependence of past events to define the current events. Particularly, the calibration of prices of different markets showed

good results when they were fitted by a trend component of order zero and autoregressive (AR) orders all equal to 1. But the difference lay on the seasonality and the moving-average (MA) orders. In the case of seasonality, we obtained good results when it was modeled with periodicity $(24, 24, 24, 20, 17, 13, 9, 24)$, referring to the day-ahead, the six intraday, and the imbalance markets, respectively. In all cases, we fixed the periodicity according with the duration (in hours) of each market. (We stress out that we removed the inactive periods from the time series of the incomplete intraday markets before calibration, thus transforming the data into continuous time series.) Referring to the MA coefficients, we arrived at the conclusion that the most parsimonious and regular way to model them was by introducing lags at 1, 2, and the periodicity. This procedure would indicate that the fourth intraday market price, active over a 17-hour period, was best modeled by an ARMA component with AR lag equal to 1 and MA lags 1, 2, and 17. This provided in all markets and months (save for the imbalance, which required an additional lag at 3) a reasonably good response in the acutocorrelation and partial autocorrelation plots, as shown in Fig. 4.

The only concerns might be with the residuals of some models. In some cases, the residuals showed reduced skewness, but a high kurtosis. That is, the residuals failed to completely satisfy the normality assumption, which was also confirmed by the Anderson–Darling test. Hyndmand *et al.* discussed this issue (the excess kurtosis or "peakedness" of residual distributions) in [39, §9.3], and they concluded that it may be attributed to outliers. In this respect, they stressed that extended models that allow for those outliers producing the excess kurtosis might have a minor effect upon the estimates. So in order to keep the model simple, we accepted the parameter estimate; mindful that, were the outliers represented by a more complex model based for instance on Student's t innovations, the marginal improvement in the model estimate would be minimal.

In addition to the residual tests, it is instructive to see how the simulations obtained by the structural model show the original characteristics of the input series. The plots of Fig. 5 exemplify how the simulated series replicate characteristics such as the seasonality, amplitude, and variance. This figure can be compared to the left panel (specifically January data) in Fig. 7, where the original data distribution is shown. Imbalance market is prone to major oscillations, as well as variability, as shown in Fig. 7. This is clearly reproduced by simulating the model, in the bottom panel of Fig. 5. Oscillation amplitude and apparent volatility are lower in the day-ahead market. Finally, the fourth intraday market is similar to the day-ahead, but with a slightly higher mean value in Fig. 7, which can be also qualitatively estimated by comparing the top and middle panel of Fig. 5.

Noticeably, the simulations of the three time series produced quite different patterns. Importantly, markets have shown remarkably distinctive patterns, what implies that a common model cannot be used to formulate the behavior of all markets. Though we have stressed out the advantages of employing a single structured methodology to facilitate and standardize the modeling of markets and wind, it is evident from this results that the calibration must be conducted for separate models (see the above discussions about the selection of periodicity and MA lags).

Fig. 7 also indicates how the eight-market price data distributions are summarized into one equivalent market distribution. A first interpretation is that the result depends on the activation time of each market. Thus, it is apparent from Fig. 7 that the last intraday markets—which are inactive for a number of hours

every day—have a consequent lower impact on the resulting distribution. The generally higher prices compared to the day-ahead market do not directly increase the combined price. Also, the results in Fig. 7 show that the imbalance market have not a large impact on the resulting distribution. This is a curious result, when we know that the imbalance market, unlike the last intraday markets, is constantly active. However, the explanation to this effect may be in that the imbalance price is a combination of two prices, λ_t^+ and λ_t^-, which are neither constantly nor simultaneously different from the day-ahead price. This means that their impact is not so marked as it would be expected from their high volatility.

Fig. 8 illustrates how the algorithm calculates the optimal switching actions, and how the sequence required for optimal income is complex under the combined market framework. The top panel shows a distorted evolution of prices, with frequent spikes revealing the real-time need for adjustment in the imbalance market. This distorted evolution in the vertical axis is also distorted in the horizontal axis, where the sample numbers have no direct resemblance to the time. At peak hours, there is an accumulation of active markets, which makes that eight consecutive samples represent one dispatch hour. At other times, one hour will result in five samples in Fig. 8. Regardless, the underlying price components, trend and seasonality, are still readily visible. This is important, because the composition of prices to obtain the series in the top panel reflects the sequence of prices that the market participants observe as a function of each sequence of dispatch hours. This makes it possible to apply the optimization algorithm coherently, when every price is next to the price that in a real sequence would be observed.

Around sample 2600 the switching was vigorous with peaks reaching 1260 kW, which is the combined rated power of the wind generator and the ESS. This reflects the advantages of operating at a period in which prices are high and also all markets are active. Around sample 2900, however, the ESS was inactive, and the power traded was only that produced by the wind generator. This may seem strange at first, because prices where the highest, due to a short system during peak time. It demonstrates, however, that the algorithm correctly decides an operation based on past history. Before sample 2600 there were sharp falls in prices, corresponding to long positions of parties that in an already long system received very low prices. The algorithm observed this as (i) an uninteresting price to sell energy, and consequently (ii) a good opportunity for charging the ESS. When sample 2600 was nearing, the ESS was optimally charged from that previous operation in the imbalance market and ready to sell under the more attractive prices. Before sample 2900 there were not such previous low prices that would deem the ESS charging profitable, and therefore the algorithm acted differently and decided that the optimal solution was to sell all the production (low or high) at the high prices. Once the prices started to fall in all eight markets after sample 2900, the ESS was progressively charged and discharged through successive hours and markets, so that just before sample 3000, when again prices were the highest, the combined power again went up to almost 1200 kW.

Under this situation, the analysis of the conditional mean of the optimal income as a function of the market prices offers guidance about how the market structure and the bidding policy are related. We refer to the results in Table 2 in order to conduct this discussion. These results must be interpreted with caution, nonetheless, because they predict only a reduced proportion of the income variance. This stems from the practically null correlation between wind speed and prices at the individual wind power generation level, as well as the basic assumption that the wind producer is a price-taker. In any case, our aim has not been

to provide an accurate model of the income as a function of the price evolution and the bidding options, but to offer a classification and identification of some of the statistically significant factors affecting that income. Nevertheless, we shall keep an eye on the value of R^2 precisely because it shows how the addition of ESS improves the control of such variability by the bidding agent. Above all, we are aware that a simple regression model does not capture the complex interactions of most of the variability. Nonlinear regression with interaction effects proved to improve the models, but at the cost of complicating the result interpretation, which herein is focused on reveling the improvements achieved by introducing ESS and the validity of the approach.

The base or benchmark case is represented in column (1) of Table 2, and it serves to highlight the main features of interest by which we can characterize a wind power producer operating under the analyzed market structure. This is the case when the producer offered all the available power in the day-ahead market. As expected, the day-ahead coefficient, $+0.44$, indicates a high positive effect resulting from price rises. Still significant is the first intraday market coefficient, which shows a small negative impact. Presumably this is but an spurious result, because the bid in this case was null for this market since the full forecast power was offered in the day-ahead market.

Case (2) confirms the usefulness of the day-ahead coefficient as an indicator of the "quality" of the generation in relation to the market price structure. The turbine employed in (2) had a reduced range of usable wind speed compared to case (1). So it was expected that it would miss good market conditions more often than the turbine in case (1). And this is revealed by the drop in the day-ahead coefficient. This conclusion may be extended to the analysis of other cases in which those good trading opportunities are missed. That is the situation of case (3), which addressed the shape of the wind speed probability distribution. The combination of high skewness—meaning a less symmetric distribution—and a low mean speed, resulted in a marked drop of the day-ahead coefficient, again because of the reduction in importance of prices when simply there is less energy available. In both cases, (2) and (3), the drop in the day-ahead coefficients, compared to (1), is additionally corroborated by the fall of mean income (see bottom row of Table 2).

The results of case analysis (4) are different from those of the previous cases. In this case, the wind power producer in (1) was allowed to correct the bidding positions as uncertainty progressively revealed. We obtained a sample of power forecast based on a Normal distribution with mean equal to the simulated power path and variance progressively decreasing as the time approached that of the real dispatch. The day-ahead importance is almost the same as in (1), which could be attributed to the low benefit from corrections in markets following the day-ahead. The negligibly difference, not only in the day-ahead coefficient but also in the received income, may stem from a combination of the small price difference between day-ahead and following marketts and the size of the corrections as the uncertainty is progressively reduced.

Finally, the results of case (5) show that the effect of price composition and distribution on the values of the day-ahead coefficient and the mean income is different in magnitude. In (5) the prices were from April 2017, which showed lower than those of January in case (1) (see Fig. 7). As a consequence the mean income dropped by a 40%. However, the variation of the day-ahead coefficient was only a 9%. Because the day-ahead coefficient accounts for the *explained* variability of income due to the variations of price, it

does not explain a large portion of the obtained income, which in this case results in a profitability loss unexplained by the basic regression model.

The results in columns (6)–(8) were obtained after incorporating energy storage. As a direct consequence, the rise of the adjusted R^2 in the results of Table 2 is substantial. We argue that this may be justified by the improvement in energy control, attributable to the ESS, which reduced the unexplained part of the model. Indeed, we observed that, all other things being constant, an increase in the ESS capacity—and consequently in the control capability—induced a further increase of R^2.

Also, it is remarkable that the coefficients of intraday and imbalance prices are now significant. This must not come as a surprise, because in these cases the power traded in those markets was not null. But it did drew our attention the ubiquitous occurrence of negative values, implying that a rise of the price would force a reduction of income. At first, this seems really counterintuitive. However, in our opinion this shows indirectly the preference of the algorithm for some more profitable markets in a setting were available power is bounded over the duration of the hourly trading. The available power at the beginning of each hour would be the sum of the wind power forecast plus the energy stored from the previous hour. This poses a limit on the energy available for sale during the eight markets of every hour. Purchases and sales of stored energy would occur in the intraday markets (see Fig. 8), but importantly the amount of energy available for sale would be bounded by the energy available in the day-ahead market *and* the purchases on intermediate markets. Seen from this perspective, an increase of the price of energy in an intermediate market where comparatively the purchase of energy is more profitable would have a *negative* effect on global income.

The above explanation may serve to put an interpretation to the results from the optimal switching policy calculated by the proposed algorithm. Case (7) is comparable to (5), the April 2017 analysis, but with storage considered in the analysis. Clearly in this case the day-ahead market had the largest impact on income. This demonstrates—when compared to (1), (5), and (6)—that low prices along with low variance and low differences between market prices, produce an optimal switching policy that favors high sales on the day-ahead, successive purchases in intraday markets, and a final sale in the imbalance market. When prices are higher, more volatile, and show larger price corrections between markets, like in case (6), not all intraday markets would be used preferentially as purchasing markets. Similar conclusions would be achieved with case (8) when compared to (4).

Other analyzed cases, not reported here for brevity, gave similar results. Overall when ESS was used, the use of intraday markets was primarily for purchasing energy. Day-ahead and imbalance markets always showed to be used mainly for selling energy. Variations on the power production—by narrowing the range of usable wind speed by the wind turbine or by using less favorable wind profiles—mainly modified the preferred use of the first intraday markets. But the conclusions were similar to those discussed above.

Finally, it is worth noting the improvements in mean income obtained by using ESS to support wind power production. Using January 2017 data, when prices were relatively high, with also high volatility, the mean income increased from 138,900 to 141,100 €. In April 2017 the increment was from 82,400 to 84,500 €. That means, respectively, 1.5% and 2.5%. To achieve this relatively small increments, the ESS was rated to 1200 MWh, which implied that it had to have the capacity to provide the full wind turbine power over a

two-hour period. These small values could be attributed to the relatively small margins observed between the prices of day-ahead and intraday markets. Imbalance market is more volatile, but as we noted above, its activation periods and sign strongly affect the profits. An analysis of the economic viability should be necessary.

5. Conclusion

This paper has examined results from the combined operation of wind power and energy storage in a multi-stage electricity market. The aim has been to determine the economic value that ideally might be achieved if that operation were optimal. To that purpose, it has been shown that the problem can be approached as a stochastic optimization dynamic program, in which samples of wind power and market prices are analyzed sequentially, allowing for energy storage decisions to be taken At the heart of this approach is a condensation of the market prices into a single time series that, along with an incremental view of submitted power, simplifies the design of the dynamic program. Because decision must be made under uncertainty, those prices cannot be just historical records. This paper has shown how they can be modeled by means of a common DLM structure that can be customized for each market price series. As a result, hundreds of price realizations can be obtained that have statistical significance and provide a framework to analyze the expected value of the optimal operation.

The presented approach has been used in this paper to analyze the value of operation in the Spanish electricity market, which consists of a day-ahead, six intraday, and an imbalance market (plus some other auxiliary markets not considered here). Different scenarios have been considered: varying amounts of captured wind energy, forecast improvements, price levels, and of course the use of ESS. The analysis of the such disparate situations has been conducted by means of a simple multiple linear regression. On the whole, the multiple linear regression is not the most adequate tool to model the complex interactions between prices and received income. More involved machine learning methods would be needed to obtain models that would be acceptable for producing predictions. This is clearly out of the scope of this paper. But the simple regression model employed has shown to be a fairly good tool to spot changes introduced by the configuration of the bidding policy and the gains introduced by an optimally switched ESS. Visibly, little of the variability was explained by the regression model when no ESS was present. But this was a clear consequence of the little or null control that can be exerted over a generator with uncertain production. Regardless, in these cases the regression analyses spotted the more advantageous cases—better wind regime and wind turbine—by producing a larger value of explained variability and a larger coefficient of the day-ahead market. When ESS was analyzed, this result was emphasized. The regression showed larger adjusted R^2 and, interestingly, it classified the market activity. We claim that the signs and values of the regression coefficients serve as an indication of the preferred markets, for selling or purchasing energy. The analyses showed, particularly, how depending on the setting the intraday markets were preferably used as purchasing markets in order to charge the ESS. Mostly this seems to be true in the last intraday markets. However, the use of the first intraday markets appeared to depend on factors such as the wind forecast accuracy and the potential profit; which in turn depend on the price levels and power production.

Overall, our analysis has shown that participation in intraday markets using ESS does not produce significant increments in income. Only around a 2%. But of course we have only dealt with the energy markets in the hourly sequence. Additional capacity, restrictions, and other ancillary services payments should be taken into account in an expanded analysis. Moreover, this paper has addressed the case of a single generator, in order to focus on the calculation procedures. It seems very reasonable that an expanded analysis aimed at studying wind powers plants, where power oscillations are to some extent damped by the lack of complete correlation, might provide better results.

References

[1] Q. Wang, C. Zhang, Y. Ding, G. Xydis, J. Wang, J. Østergaard, Review of real-time electricity markets for integrating Distributed Energy Resources and Demand Response, 2015.

[2] A. J. Conejo, M. Carrion, J. M. Morales, Decision making under uncertainty in electricity markets, Springer, New York, 2010.

[3] V. Guerrero-Mestre, A. A. Sanchez de la Nieta, J. Contreras, J. P. S. Catalao, Optimal Bidding of a Group of Wind Farms in Day-Ahead Markets Through an External Agent, IEEE Transactions on Power Systems 31 (2016) 2688–2700.

[4] P. Pinson, C. Chevallier, G. N. Kariniotakis, Trading Wind Generation From Short-Term Probabilistic Forecasts of Wind Power, IEEE Transactions on Power Systems 22 (2007) 1148–1156.

[5] H. Shin, D. Lee, R. Baldick, An Offer Strategy for Wind Power Producers That Considers the Correlation between Wind Power and Real-Time Electricity Prices, IEEE Transactions on Sustainable Energy 9 (2018) 695–706.

[6] A. Botterud, Z. Zhou, J. Wang, R. J. Bessa, H. Keko, J. Sumaili, V. Miranda, Wind power trading under uncertainty in LMP markets, IEEE Transactions on Power Systems 27 (2012) 894–903.

[7] T. K. Boomsma, N. Juul, S. E. Fleten, Bidding in sequential electricity markets: The Nordic case, European Journal of Operational Research 238 (2014) 797–809.

[8] L. Baringo, A. J. Conejo, Offering Strategy of Wind-Power Producer: A Multi-Stage Risk-Constrained Approach, IEEE Transactions on Power Systems 31 (2016) 1420–1429.

[9] E. Y. Bitar, R. Rajagopal, P. P. Khargonekar, K. Poolla, P. Varaiya, Bringing Wind Energy to Market, IEEE Transactions on Power Systems 27 (2012) 1225–1235.

[10] M. Bueno-Lorenzo, M. Á. Moreno, J. Usaola, Analysis of the imbalance price scheme in the Spanish electricity market: A wind power test case, Energy Policy 62 (2013) 1010–1019.

[11] J. García-González, R. M. R. de la Muela, L. M. Santos, A. M. Gonzalez, Stochastic joint optimization of wind generation and pumped-storage units in an electricity market, IEEE Transactions on Power Systems 23 (2008) 460–468.

[12] A. A. S. De La Nieta, J. Contreras, J. I. Muñoz, Optimal coordinated wind-hydro bidding strategies in day-ahead markets, IEEE Transactions on Power Systems 28 (2013) 798–809.

[13] F. de Bosio, V. Verda, Thermoeconomic analysis of a Compressed Air Energy Storage (CAES) system integrated with a wind power plant in the framework of the IPEX Market, Applied Energy 152 (2015) 173–182.

[14] J. Moradi, H. Shahinzadeh, A. Khandan, M. Moazzami, A profitability investigation into the collaborative operation of wind and underwater compressed air energy storage units in the spot market, Energy 141 (2017) 1779–1794.

[15] I. L. Gomes, H. M. Pousinho, R. Melício, V. M. Mendes, Stochastic coordination of joint wind and photovoltaic systems with energy storage in day-ahead market, Energy 124 (2017) 310–320.

[16] M. S. Al-Swaiti, A. T. Al-Awami, M. W. Khalid, Co-optimized trading of wind-thermal-pumped storage system in energy and regulation markets, Energy 138 (2017) 991–1005.

[17] A. Berrada, K. Loudiyi, I. Zorkani, Valuation of energy storage in energy and regulation markets, Energy 115 (2016) 1109–1118.

[18] L. Bayón, J. M. Grau, M. M. Ruiz, P. M. Suárez, A comparative economic study of two configurations of hydro-wind power plants, Energy 112 (2016) 8–16.

[19] M. Khalid, R. P. Aguilera, A. V. Savkin, V. G. Agelidis, On maximizing profit of wind-battery supported power station based on wind power and energy price forecasting, Applied Energy 211 (2018) 764–773.

[20] OMIE's data repository, http://www.omie.es/aplicaciones/datosftp/datosftp.jsp, 2018. Accessed: 2018-04-20.

[21] NREL's data repository, https://www.nrel.gov/grid/western-wind-data.html, 2018. Accessed: 2018-04-20.

[22] J. Durbin, S. J. Koopman, Time Series Analysis by State Space Methods: Second Edition, Oxford University Press, 2012.

[23] R. Panda, T. Sarkar, A. Bhattacharya, Stochastic study of the wind-energy potential of India, Energy 15 (1990) 921–930.

[24] O. Grothe, J. Schnieders, Spatial dependence in wind and optimal wind power allocation: A copula-based analysis, Energy Policy 39 (2011) 4742–4754.

[25] C. Delgado, J. Domínguez-Navarro, Point estimate method for probabilistic load flow of an unbalanced power distribution system with correlated wind and solar sources, International Journal of Electrical Power & Energy Systems 61 (2014) 267–278.

[26] A. Papavasiliou, S. S. Oren, R. P. O'Neill, Reserve requirements for wind power integration: A scenario-based stochastic programming framework, IEEE Transactions on Power Systems 26 (2011) 2197–2206.

[27] J. Morales, R. Mínguez, A. Conejo, A methodology to generate statistically dependent wind speed scenarios, Applied Energy 87 (2010) 843–855.

[28] Z. Qin, W. Li, X. Xiong, Incorporating multiple correlations among wind speeds, photovoltaic powers and bus loads in composite system reliability evaluation, Applied Energy 110 (2013) 285–294.

[29] G. Diaz, E. Planas, A Note on the Normalization of Spanish Electricity Spot Prices, IEEE Transactions on Power Systems PP (2015) 1–2.
[30] R. Zárate-Miñano, M. Anghel, F. Milano, Continuous wind speed models based on stochastic differential equations, Applied Energy 104 (2013) 42–49.
[31] Z. I. Botev, J. F. Grotowski, D. P. Kroese, Kernel density estimation via diffusion, The Annals of Statistics 38 (2010) 2916–2957.
[32] F. E. Benth, V. A. Kholodnyi, P. Laurence, Quantitative energy finance: Modeling, pricing, and hedging in energy and commodity markets, 2014.
[33] S. T. Rachev, Y. S. Kim, M. L. Bianchi, F. J. Fabozzi, CFA, Financial Models with Levy Processes and Volatility Clustering, John Wiley & Sons, 2011.
[34] R. Bellman, Dynamic Programming, Courier Corporation, 2013.
[35] F. A. Longstaff, E. S. Schwartz, Valuing American options by simulation: a simple least-squares approach, Review of Financial Studies 14 (2001) 113–147.
[36] M. Yoder, A. S. Hering, W. C. Navidi, K. Larson, Short-term forecasting of categorical changes in wind power with Markov chain models, Wind Energy 17 (2014) 1425–1439.
[37] T. P. Chang, Performance comparison of six numerical methods in estimating Weibull parameters for wind energy application, Applied Energy 88 (2011) 272–282.
[38] L. Lu, H. Yang, J. Burnett, Investigation on wind power potential on Hong Kong islands—an analysis of wind power and wind turbine characteristics, Renewable Energy 27 (2002) 1–12.
[39] R. J. Hyndman, Forecasting with Exponential Smoothing: The State Space Approach, Springer Berlin Heidelberg, 2008.